MICROSTRUCTURES

Sequence-encoded colloidal origami and microbot assemblies from patchy magnetic cubes

Koohee Han,[1,2] C. Wyatt Shields IV,[2,3] Nidhi M. Diwakar,[2] Bhuvnesh Bharti,[1,2]* Gabriel P. López,[2,3,4†‡] Orlin D. Velev[1,2‡]

Colloidal-scale assemblies that reconfigure on demand may serve as the next generation of soft "microbots," artificial muscles, and other biomimetic devices. This requires the precise arrangement of particles into structures that are preprogrammed to reversibly change shape when actuated by external fields. The design and making of colloidal-scale assemblies with encoded directional particle-particle interactions remain a major challenge. We show how assemblies of metallodielectric patchy microcubes can be engineered to store energy through magnetic polarization and release it on demand by microscale reconfiguration. The dynamic pattern of folding and reconfiguration of the chain-like assemblies can be encoded in the sequence of the cube orientation. The residual polarization of the metallic facets on the microcubes leads to local interactions between the neighboring particles, which is directed by the conformational restrictions of their shape after harvesting energy from external magnetic fields. These structures can also be directionally moved, steered, and maneuvered by global forces from external magnetic fields. We illustrate these capabilities by examples of assemblies of specific sequences that can be actuated, reoriented, and spatially maneuvered to perform microscale operations such as capturing and transporting live cells, acting as prototypes of microbots, micromixers, and other active microstructures.

INTRODUCTION

Miniaturized and soft robotic devices for biological micromanipulation, cell-level diagnosis, drug delivery, and microsurgery are typically made by reductive ("top-down") microfabrication (*1*–*6*) but could be made much more efficiently by microscale self-assembly (*7*, *8*). Assemblies of colloidal particles with well-defined shape, orientation, and response to external stimulation can form the basis of simple responsive materials (*9*–*19*), yet endowing them with more complex functionality has been challenging (*7*, *8*). The primary challenges in realizing these active structures include the remote supply of energy, control over their response, and directional translocation (*20*, *21*). One way to overcome these challenges is to make assemblies from colloidal particles with tailored form factors and surface polarizabilities (*22*–*26*). We have previously shown that anisotropically shaped metallic patchy particles can acquire complex polarization patterns in electric and magnetic fields, leading to multidirectional interactions and to the formation of assemblies of unusual structure and symmetry (*27*). Here, we describe and analyze the emergent, sequence-specific, self-reconfiguration dynamics in supracolloidal assemblies of cube-shaped particles with one metal-coated facet.

RESULTS AND DISCUSSION

Magnetic field assembly and actuation of multicube clusters

We applied intermittent external magnetic fields to drive the assembly of patchy microcubes of edge length ~10 μm, where one face of the microcube is selectively coated with 100 nm of cobalt (Co) metal (see Materials and Methods). When a uniform magnetic field of 0.1 to 10 kA/m is generated (for example, by a collinear pair of electromagnets, as shown in Fig. 1A) and applied across a chamber containing an aqueous suspension of randomly dispersed microcubes, the magnetic patch on each cube acquires a dipole leading to long-range attraction between the cubes, and chain assembly (see the Supplementary Materials for more details on the assembly process with statistical analysis). The magnetized microcubes assemble into stretched chain configurations oriented along the direction of the applied magnetic field (*27*), as shown in Fig. 1 (B and C). The organization in chains is the result of the dipole-dipole attraction between the magnetic patches on the microcubes (*27*, *28*). The role of the magnetic coating as a structural director of the chains is confirmed through imaging with energy-dispersive spectroscopy (EDS; fig. S1). The ferromagnetic nature of the Co patches (fig. S3) allows for the storage of magnetic energy to locally guide the particle-particle interactions in the absence of an applied magnetic field for reconfiguration (Fig. 1D) while conserving the overall sequence of cubes within the assembly.

The focus of this report is the unusual dynamic rearrangement of the assembled chains of microcubes into partially wrapped and bundled states every time the field is toggled on or off. One example of such dynamics is shown in Fig. 1 (C and D) and movie S1. This phenomenon originates from the change in configurational energy of the assembled chain, which can be divided into two major components: (i) dipole-field and (ii) dipole-dipole interaction energies. The dipole-field interaction predominates in the presence of the external field, which extends the dipolar chain into a stretched linear configuration (Fig. 1C). Upon eliminating this field, the quasi-equilibrium configuration is governed by the residual dipole-dipole interaction energies, resulting in a collapsed, self-folded structure (Fig. 1D). As we explain in detail below, the pattern of this rearrangement is determined by the sequence of the patchy cubes with coated sides facing in the same or opposite direction along the chain (analogically to "cis/trans" orientations).

To understand the driving forces and control the self-reconfiguration of patchy microcube chains, we first analyze the interactions between microcube doublets. The two basic sequence units attained by a doublet are shown in Fig. 1E. We refer to the sequence as *AB* when the cube body

[1]Department of Chemical and Biomolecular Engineering, North Carolina State University, Raleigh, NC 27695–7905, USA. [2]Research Triangle Materials Research Science and Engineering Center, Durham, NC 27708, USA. [3]Department of Biomedical Engineering, Duke University, Durham, NC 27708, USA. [4]Department of Mechanical Engineering and Materials Science, Duke University, Durham, NC 27708, USA.
*Present address: Cain Department of Chemical Engineering, Louisiana State University, Baton Rouge, LA 70803, USA.
†Present address: Department of Chemical and Biological Engineering, University of New Mexico, Albuquerque, NM 87131, USA.
‡Corresponding author. Email: odvelev@ncsu.edu (O.D.V.); gplopez@unm.edu (G.P.L.)

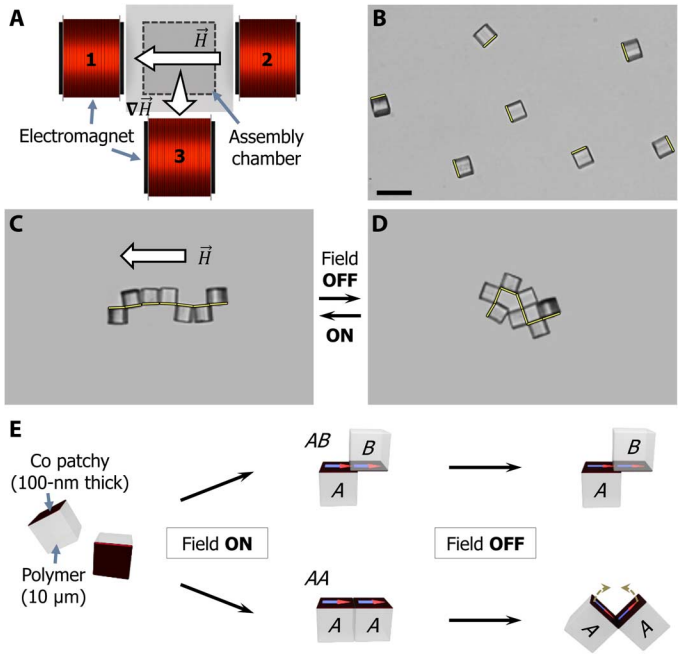

Fig. 1. Magnetic field–driven assembly of patchy microcubes and their modes of self-reconfiguration. (**A**) Schematic of the experimental setup used to assemble and manipulate the patchy microcubes. A uniform magnetic field was generated by a collinear pair of electromagnets (1 and 2), and a magnetic field gradient was imposed by a single electromagnet (3). (**B**) Micrograph of an aqueous dispersion of single-side cobalt-coated patchy microcubes (the superimposed yellow lines represent the magnetic patches; scale bar, 20 μm). (**C**) Example of a linear chain of patchy microcubes formed upon the application of a uniform magnetic field. (**D**) Reversible self-reconfiguration of the linear chain in (C) into a structure of two closed loops upon removing the applied field (movie S1). (**E**) Schematics of the assembly pathways for the two basic unit doublets, *AA* and *AB*, which correspond to assembled particles on the same side and opposite sides of the assembled magnetic films, respectively.

of the two adjacent microcubes is on the opposite side of the plane of metal patches, and conversely, *AA* denotes a sequence of two cubes on the same side of the metal plane. Depending on the type of doublet (that is, *AA* or *AB*), the energetics of the magnetic dipolar interactions upon removing the external field leads to two distinct responses, which can be modeled on the basis of two independent finite dipoles (see the Supplementary Materials) (*29*, *30*). In the case of an *AB* sequence, the two adjacent microcubes form a rigid link due to partial overlap between the metallic patches, whereby two adjoining residual dipoles have minimized their interaction energy, resulting in rigid bonding (Fig. 1E, top). In contrast, when the metallic patches are on the same side, as in the *AA* sequence, the magnetic interaction energy between the residual dipoles is minimized by self-folding of the doublet along the common vertex when the external field is removed (Fig. 1E, bottom).

Rules of self-folding driven by residual dipolar interactions

A variety of self-reconfiguring and actuating structures could be obtained by programming the sequence of *AB* and *AA* configurations along a larger chain-like assembly. To analyze this phenomenon, first we focus on the change in the dipole-dipole interaction energy of small cluster ensembles (that is, *AA*, *AAA*, and *AAB*). The common point-dipole approximation is not suitable for evaluation of the energy of these ensembles because when the ensembles self-fold into their ground state, the mean distance between the centers of each magnetic patch becomes much smaller than the patch length (*29*, *30*). To ensure that the magnitude of the configuration energy is within a realistic range for all possible configurations, we analytically calculated the magnetostatic energy of a multicube cluster using a finite-length dipole interaction model between the polarized metallic patches on each microcube. The generic equation for estimating the interaction energy (E_{int}) between dipoles with the length of $2l$ is given as (*29*, *30*)

$$E_{int} = \frac{\mu_0}{4\pi}\left(\frac{m}{2l}\right)^2 \sum_{x=1}^{2}\sum_{y=1}^{2}\left[\frac{(-1)^{x-y+1}}{|\vec{r}_{ij} + l\{(-1)^x \vec{n}_i + (-1)^y \vec{n}_j\}|}\right] \quad (1)$$

where μ_0 is the permeability of free space ($4\pi \times 10^{-7}$ m kg s^{-2} A^{-2}), m is the residual magnetic moment, and $\vec{r}_{ij}$ is the position vector between the centers of each dipole, $\vec{n}_i$ and $\vec{n}_j$. We assume a dipole length of 9.3(±0.4) μm, which can be estimated from scanning electron microscopy (SEM) images of assembled microcubes (fig. S1C).

In the case of the *AA* and *AAA* chain sequences, the linear microcube clusters self-fold upon removing the field (Fig. 2, A to F), reaching a state with a deep minimum of the interaction energy between the residual dipoles in the reorganized metal patches. In the simplest case, an *AA* doublet, the ground state is achieved as $|\bar{\delta}| \to 0°$, where the two adjacent dipoles are antiparallel. We refer to this structure as configuration *C* (Fig. 2C). At this configuration, the magnetized patches of the two cubes attract strongly and are inseparable by reintroduction of the external field (Fig. 2, B and C, and movie S2). The interaction of the residual magnetic dipoles in the *AAA* sequence leads to the formation of a triangular cyclic shape after the external field is removed (Fig. 2E). This structure is metastable and further collapses into the lower-energy permanent *AC* configuration upon reintroduction of the field (Fig. 2, E and F, and movie S2). The formation of these nonreconfigurable states can be averted by programming the sequence of the microcube chain to include a spatial restriction/barrier preventing its collapse into the ground state. The simplest example of this spatial restriction is encountered in the sequence *AAB*, where the steric constraint of the *AB* link physically blocks the first microcube *A* from completely closing on the second one and prevents the formation of a nonreconfigurable collapsed state, *AC* sequence. This steric restriction leads to completely reversible reconfiguration (between the states shown in Fig. 2, H and I) each time the external magnetic field is toggled on and off. This principle of directional magnetic reconfiguration can be scaled down to cubes with an edge length as small as ~200 nm, because this is the size range where the magnetic interaction energy still dominates thermal fluctuations (see the Supplementary Materials for further details).

Field-triggered dynamic reconfiguration of multicube clusters

Two key examples of dynamic reconfiguration are revealed by "isomeric" clusters of four microcubes, whose sequence encodes distinct field-triggered reconfiguration patterns (Fig. 3A). The *ABBA* assembly forms a cyclic configuration that opens and closes on demand, whereas the *BBAA* cluster symmetrically wraps and unwraps (movie S3). The dynamic paths of self-folding and field-driven unfolding are repeated with remarkable dexterity (that is, over 20 or more field-on and field-off duty cycles; fig. S5). The rate of self-folding can be tuned by the magnitude of the applied external magnetic field. For an *ABBA* sequence, for example, the folding rate is proportional to $|\vec{H}^2|$, where $|\vec{H}|$ is the strength of initially applied magnetic field (Fig. 3B). These

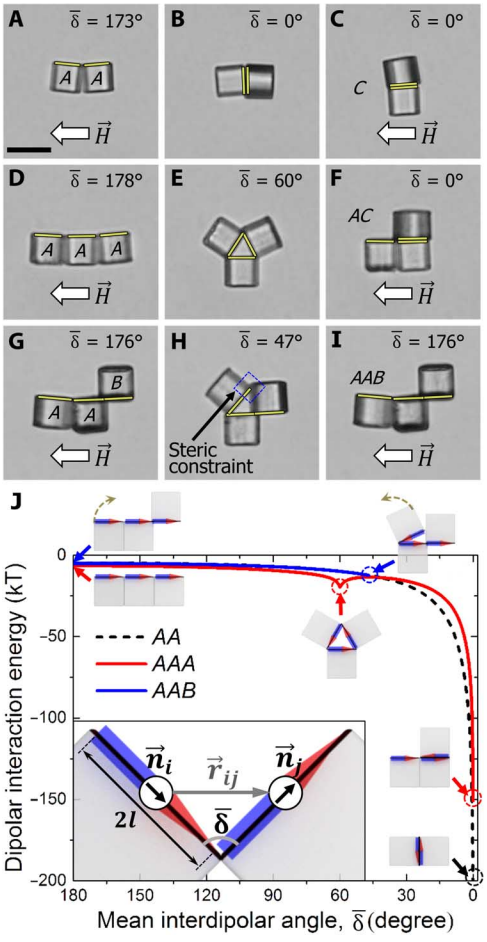

Fig. 2. Reconfiguration patterns of short chains of microcubes driven by dipole-field and residual dipole-dipole interactions. (**A** to **I**) Snapshots of the reconfiguration patterns intrinsic to *AA*, *AAA*, and *AAB* sequences. After the applied field is removed, the microcube chains self-fold (A and B, D and E, and G and H) until (i) a ground state configuration is attained [for example, (B)], (ii) a metastable structure is formed [for example, (E)], or (iii) a sterically restricted conformation is attained [for example, (H)]. When the external field is imposed again, (i) the ground state configuration *C* is retained [for example, (C)], (ii) the metastable *AAA* structure usually reconfigures into *AC* [for example, (F)], and (iii) the partially wrapped structure *AAB* reattains its initial stretched state [for example, (I)]. Scale bar, 20 μm. (**J**) Change in the magnetic dipolar energy per microcube during the reconfiguration process as a function of the interdipolar angle $\bar{\delta}$, the angle between planes of magnetic patches on adjacent microcubes, adapting self-folding toward the ground state. The inset shows the interaction between two dipoles of finite length 2*l* in terms of the unit vector of each dipole, $\vec{n}_i$ and $\vec{n}_j$, and the position vector $\vec{r}_{ij}$ between $\vec{n}_i$ and $\vec{n}_j$.

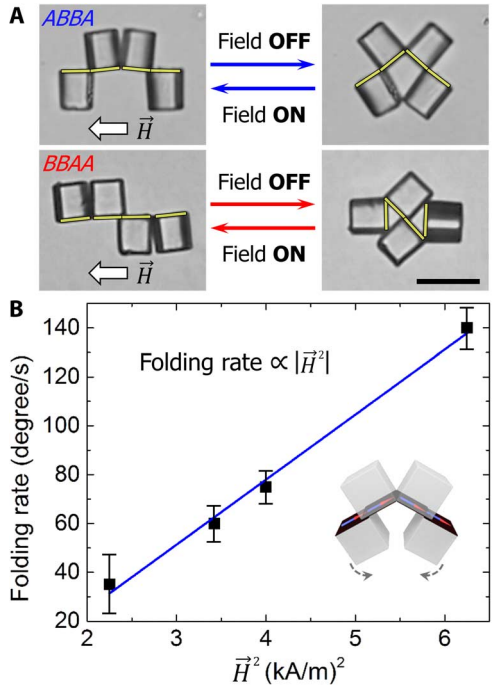

Fig. 3. Examples of dynamic reconfiguration of chain sequences comprising four microcubes. (**A**) Snapshots of field-on and field-off states of the four particle colloidal isomers (that is, *ABBA* and *BBAA*). Scale bar, 20 μm. (**B**) Dependence of folding rate measured for the initial 0.5 s of the *ABBA* microcube sequence on the applied magnetic field strength after the field is removed. The folding rate is linearly dependent on the square of the strength of initially applied magnetic field. The error bars correspond to the SD of the folding rate per the square of the field strength from five different *ABBA* structures.

dependencies are typical for second-order field-induced interactions and dynamics (*31*).

Examples of microbots and colloidal origami with sequence-encoded function

The reversible, sequence-dependent, reconfiguration described above is actuated by a uniform magnetic field. A further level of control over the dynamics of these assemblies can be achieved by superimposing a magnetic field gradient ($\nabla\vec{H}$) that can remotely translocate the assemblies. By combining the uniform field-triggered reversible actuation with field gradient–driven spatial navigation, we illustrate how a microcube assembly with a *BABBAB* sequence can form a prototype of a microbot that can manipulate single live cells. Snapshots of this microbot grabbing, transporting, and releasing a target yeast cell are shown in Fig. 4 (A to E) and movie S4. The microbot cluster is transported to the target location in its open configuration (Fig. 4A) by the application of a transversal uniform magnetic field with an imposed additional longitudinal gradient (by turning on all three coils 1, 2, and 3 in Fig. 1A). In the subsequent step, the transverse magnetic field is removed, resulting into chain self-folding into the closed state. Thus, the cluster acts as a "microtweezer" and captures the target yeast cell. The cell is then transported in two-dimensional space by tuning the magnitude and direction of the applied magnetic field gradient (Fig. 4, C and D). Upon reaching a target location, the yeast cell is released by activating the uniform magnetic field (Fig. 4E).

To verify and illustrate the origin of the dynamics of these assemblies, we simulated the different scenarios of field interaction with a *BABBAB* microbot using the COMSOL Multiphysics software package (Fig. 4, F to J). For simplicity, the calculations were carried out in two dimensions, where the three-dimensional microcube was represented as a square and the magnetic plane as a rectangular patch on one of its sides (see Materials and Methods). The calculated field distribution, plotted by color coding, elucidates the migration of the chain structure in the direction of positive magnetic field gradient (Fig. 4, F and H). This analysis confirms the role of the applied uniform magnetic field in unfolding the chain (Fig. 4, G and J) and shows that the reconfiguration of the microbot in the absence of external field is driven by strong

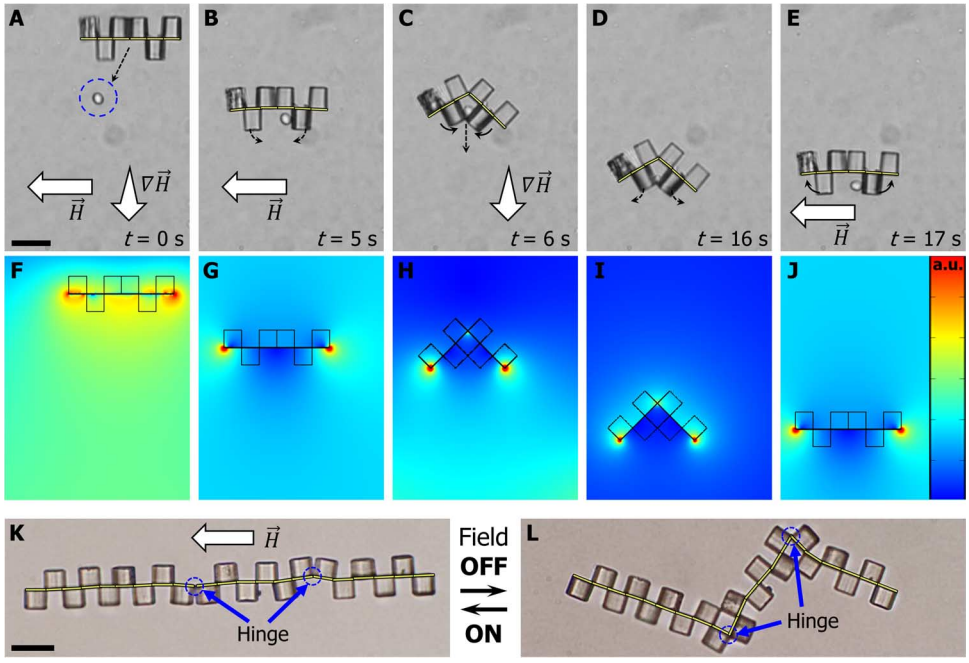

Fig. 4. Microcube assemblies as prototypes of microbots for transporting cells and as colloidal origami. (**A** to **E**) Snapshots of a microbot comprising six microcubes (*BABBAB*) used for transporting a yeast cell. (A) Spatial migration of the assembly in its open state under uniform external magnetic field with longitudinally imposed gradient. (B) The microcube chain is brought to the yeast cell by attraction along the gradient. (C) The cluster self-closes upon removing the uniform field, which results in the capture of the yeast cell. (D) The microbot is transported to the target location by a magnetic gradient force. (E) Finally, the cell is released by reactivating the uniform magnetic field. (**F** to **J**) Distribution of magnetic field intensity around the *BABBAB* assembly during each stage of manipulation shown in (A) to (E), as calculated by COMSOL Multiphysics. (**K** and **L**) Snapshots of a repeatedly self-reconfigurable multicube chain as an example of programmable colloidal origami. Scale bars, 20 μm (A and K).

cluster-localized magnetic interactions (as shown by the location of the high field intensity areas in Fig. 4, I and H).

The *BABBAB* "microbot" is one of many possible examples of small, reversibly actuatable clusters. One route to programmed assembly of these structures is magnetic rotation of the assemblies and sequential addition of single cubes to their chains. This directed addition can be achieved via magnetic torque by modulating the external field characteristics (for example, the direction and strength of the field; see figs. S5 and S6 and movies S5 and S6 for more details). In a more scalable and parallelized fabrication of these structures, an underlying template may allow the assembly of preprogramed sequences by directing the cubes onto patterned micromagnets (*32*). A larger-scale application of longer "origami" chains could involve embedding reversibly collapsible chains within flexible matrices for making responsive materials that can be expanded, contracted, or folded by magnetic fields. We present one example of these reconfigurable chains in Fig. 4 (K and L). As highlighted by the blue circles (Fig. 4, K and L), the folding behavior is consistently observed at either the *AA* or *BB* "hinge" segments, even within a large cluster.

CONCLUSIONS

We demonstrate how microcubes with one metal-coated side can be assembled into structures that store and release magnetic energy when the steric constraints of their cubic building blocks guide their residual magnetic interactions. These assemblies attain various equilibrium and nonequilibrium states, depending on the sequence of the microcubes, which make it possible to program their self-folding and wrapping patterns. Field-manipulated microbot clusters with sequence-determined folding pattern and function (Fig. 4) may find utility in soft robotics, microsurgery, biological separation, and bioinspired colloidal origami (*33*). In addition to biological manipulations on the microscale, these assemblies can be used to locally probe and interact with their microenvironment. Preliminary studies not reported here show that reversible self-reconfiguration of specific microcube chains could lead to new classes of "active" microswimmers and novel microrheometers for non-Newtonian or biological media. Because the engineered metallic patches provide a foundation for effective magnetic energy storage, the principles of this simple platform actuator can be extended to more advanced, hierarchical structures by using more complex particle shapes, compositions, and field parameters to address a broad range of applications, from robotics and micromanipulation to responsive materials and on-demand reconfigurable structures.

MATERIALS AND METHODS

Sample preparation

One-side coated patchy microcubes, composed of polymer and thin cobalt (Co) films deposited along one of the six facets, were fabricated using standard photolithography and metal deposition techniques (*27*). SU-8 10 photoresist (MicroChem) was spin-coated on a 3-inch single-side polished silicon (Si) wafer (Addison Engineering Inc.) and exposed to ultraviolet (UV) light (365 nm, MA/BA6 mask aligner, SÜSS MicroTec AG) through a chrome-patterned photomask (consisting of an array of 10-μm transparent squares with a 20-μm pitch; Photo Sciences Inc.) to form the microcubes, which were revealed after development of the photoresist (following the procedures by MicroChem). Note that the fabricated microcubes can sometimes display slightly

rounded edges due the resolution of chrome-printed photomask or due to the inadequate exposure of UV light through the photomask. The wafer was then mounted inside of an electron beam metal evaporator (Solution E-Beam, CHA Industries) to allow for the deposition of 10 nm of Cr followed by 100 nm of Co on the topside of the wafer. The patchy microcubes were then harvested from the wafer by the application of shear forces from a rubber scraper and dispersed in Milli-Q water, containing 0.1 volume % Tween 20 (Sigma-Aldrich).

Experimental setup

A 30-μl solution of the patchy microcubes was placed into the assembly chamber (Fig. 1A), where a hydrophobic ring secured a 20- to 30-μm gap between a glass slide and a coverslip. A collinear pair of electromagnets (1 and 2) placed on either side of the assembly chamber generated a uniform magnetic field in the range of 0.1 to 10 kA/m, and a single electromagnet (3) placed on the bottom side of the assembly chamber generated a magnetic field gradient in the range of 1 to 100 kA/m^2, as measured by a gauss meter (GM2, AlphaLab Inc.). The assembly chamber was housed on the table of an optical microscope (BX61, Olympus) to enable the observation of the field-directed assembly and manipulation of patchy microcubes. Videos were taken using a charge-coupled device camera (DP70, Olympus) at 15 frames per second. The videos were analyzed in ImageJ (National Institutes of Health) to measure the interdipolar angle between metallic facets on adjacent particles within an assembly.

COMSOL Multiphysics simulation

Magnetostatic calculations were performed using the AC/DC module of COMSOL Multiphysics modeling software (COMSOL Inc.) to investigate the local magnetic field distribution around an assembled chain of patchy microcubes under various configurations. The magnetic permeability of the Co coating (1.1676×10^{-1} H/m), the SU-8 polymer (1.257×10^{-6} H/m), and the surrounding water medium (1.257×10^{-6} H/m) were incorporated into the model, where H (henry) is the SI unit for electrical inductance. The geometry of the system was confined to a two-dimensional area (200 μm × 200 μm) with an extremely fine triangular mesh at the center of the assembly chamber. The simulations were performed by solving Maxwell's equations with a fully coupled linear solver.

SUPPLEMENTARY MATERIALS

Supplementary material for this article is available at http://advances.sciencemag.org/cgi/content/full/3/8/e1701108/DC1

Supplementary Results and Discussion

fig. S1. An example set of images from an optical microscope, an SEM, and an SEM with an EDS overlay of an assembled chain of patchy microcubes.

fig. S2. Example of the assembly of patchy microcubes under a uniform magnetic field.

fig. S3. Magnetic hysteresis curve of a collection of dried Co-coated patchy microcubes.

fig. S4. Calculation of the dipole-dipole interaction energy for patchy microcube doublets as a function of bending angle in the absence of an external magnetic field.

fig. S5. The kinetics of the self-reconfiguration of four particle clusters expressed by mean interparticle (≡ interdipolar) angle δ.

fig. S6. Chain reorientation techniques for reprogramming the relative sequence of a microbot assembly (*BAA→BBA→ABB*).

fig. S7. Chain reorientation technique to program the sequence of a microbot.

movie S1. Magnetic field–driven actuation of an assembled chain.

movie S2. Self-folding and irreversible transition of assembled chains with sequences of *AA*, *AAA*, and *AAAA*.

movie S3. Reversible actuation of chains with sequences of *ABBB*, *ABBA*, and *BBAA*.

movie S4. Cell capture and transport by a microbot prototype.

movie S5. *BAA→BBA→ABB* chain conversion process.

movie S6. Programmed assembly of a chain with an *ABBA* sequence.

References (*34*, *35*)

REFERENCES AND NOTES

1. R. F. Shepherd, F. Ilievski, W. Choi, S. A. Morin, A. A. Stokes, A. D. Mazzeo, X. Chen, M. Wang, G. M. Whitesides, Multigait soft robot. *Proc. Natl. Acad. Sci. U.S.A.* **108**, 20400–20403 (2011).
2. E. Brown, N. Rodenberg, J. Amend, A. Mozeika, E. Steltz, M. R. Zakin, H. Lipson, H. M. Jaeger, Universal robotic gripper based on the jamming of granular material. *Proc. Natl. Acad. Sci. U.S.A.* **107**, 18809–18814 (2010).
3. W. Gao, J. Wang, Synthetic micro/nanomotors in drug delivery. *Nanoscale* **6**, 10486–10494 (2014).
4. K. Malachowski, M. Jamal, Q. Jin, B. Polat, C. J. Morris, D. H. Gracia, Self-folding single cell grippers. *Nano Lett.* **14**, 4164–4170 (2014).
5. T. S. Shim, Z. G. Estephan, Z. Qian, J. H. Prosser, S. Y. Lee, D. M. Chenoweth, D. Lee, S.-J. Park, J. C. Crocker, Shape changing thin films powered by DNA hybridization. *Nat. Nanotechnol.* **12**, 41–47 (2016).
6. Y. Liu, B. Shaw, M. D. Dickey, J. Genzer, Sequential self-folding of polymer sheets. *Sci. Adv.* **3**, e1602417 (2017).
7. L. Cademartiri, K. J. M. Bishop, Programmable self-assembly. *Nat. Mater.* **14**, 2–9 (2015).
8. S. C. Glotzer, M. J. Solomon, Anisotropy of building blocks and their assembly into complex structures. *Nat. Mater.* **6**, 557–562 (2007).
9. M. Grzelczak, J. Vermant, E. M. Furst, L. M. Liz-Marzán, Directed self-assembly of nanoparticles. *ACS Nano* **4**, 3591–3605 (2010).
10. Z. Nie, A. Petukhova, E. Kumacheva, Properties and emerging applications of self-assembled structures made from inorganic nanoparticles. *Nat. Nanotechnol.* **5**, 15–25 (2010).
11. J. Kim, S. E. Chung, S.-E. Choi, H. Lee, J. Kim, S. Kwon, Programming magnetic anisotropy in polymeric microactuators. *Nat. Mater.* **10**, 747–752 (2011).
12. J. Ge, Y. Yin, Responsive photonic crystals. *Angew. Chem. Int. Ed.* **50**, 1492–1522 (2011).
13. S. Sacanna, L. Rossi, D. J. Pine, Magnetic click colloidal assembly. *J. Am. Chem. Soc.* **134**, 6112–6115 (2012).
14. Y. Yang, L. Gao, G. P. Lopez, B. B. Yellen, Tunable assembly of colloidal crystal alloys using magnetic nanoparticle fluids. *ACS Nano* **7**, 2705–2716 (2013).
15. T.-H. Lin, W.-H. Huang, I.-K. Jun, P. Jiang, Bioinspired assembly of colloidal nanoplatelets by electric field. *Chem. Mater.* **21**, 2039–2044 (2009).
16. E. Bukusoglu, M. B. Pantoja, P. C. Mushenheim, X. Wang, N. L. Abbott, Design of responsive and active (soft) materials using liquid crystals. *Annu. Rev. Chem. Biomol. Eng.* **7**, 163–196 (2016).
17. B. Bharti, A.-L. Fameau, M. Rubinstein, O. D. Velev, Nanocapillarity-mediated magnetic assembly of nanoparticles into ultraflexible filaments and reconfigurable networks. *Nat. Mater.* **14**, 1104–1109 (2015).
18. B. Bharti, D. Rutkowski, K. Han, A. U. Kumar, C. K. Hall, O. D. Velev, Capillary bridging as a tool for assembling discrete clusters of patchy particles. *J. Am. Chem. Soc.* **138**, 14948–14953 (2016).
19. A. Kaiser, A. Snezhko, I. S. Aranson, Flocking ferromagnetic colloids. *Sci. Adv.* **3**, e1601469 (2017).
20. B. J. Nelson, I. K. Kaliakatsos, J. J. Abbott, Microrobots for minimally invasive medicine. *Annu. Rev. Biomed. Eng.* **12**, 55–85 (2010).
21. M. Sitti, Miniature devices: Voyage of the microrobots. *Nature* **458**, 1121–1122 (2009).
22. B. Bharti, O. D. Velev, Assembly of reconfigurable colloidal structures by multidirectional field-induced interactions. *Langmuir* **31**, 7987–7908 (2015).
23. J. Yan, K. Chaudhary, S. C. Bae, J. A. Lewis, S. Granick, Colloidal ribbons and rings from Janus magnetic rods. *Nat. Commun.* **4**, 1516 (2013).
24. A. A. Shah, B. Schultz, W. Zhang, S. C. Glotzer, M. J. Solomon, Actuation of shape-memory colloidal fibres of Janus ellipsoids. *Nat. Mater.* **14**, 117–124 (2014).
25. A. Snezhko, I. S. Aranson, Magnetic manipulation of self-assembled colloidal asters. *Nat. Mater.* **10**, 698–703 (2011).
26. A. Ruditskiy, B. Ren, I. Kretzschmar, Behaviour of iron oxide (Fe_3O_4) Janus particles in overlapping external AC electric and static magnetic fields. *Soft Matter* **9**, 9174 (2013).
27. C. W. Shields IV, S. Zhu, Y. Yang, B. Bharti, J. Liu, B. B. Yellen, O. D. Velev, G. P. López, Field-directed assembly of patchy anisotropic microparticles with defined shape. *Soft Matter* **9**, 9219 (2013).
28. S. K. Smoukov, S. Gangwal, M. Marquez, O. D. Velev, Reconfigurable responsive structures assembled from magnetic Janus particles. *Soft Matter* **5**, 1285 (2009).
29. M. D. Costa, Y. G. Pogorelov, Criteria for long-range magnetic order in planar lattices of dipolar coupled magnetic nanoparticles. *Phys. Status Solidi A* **927**, 923–927 (2001).
30. Y. Gu, R. Burtovyy, J. Custer, I. Luzinov, K. G. Kornev, A gradient field defeats the inherent repulsion between magnetic nanorods. *R. Soc. Open Sci.* **1**, 140271 (2014).
31. R. M. Erb, J. J. Martin, R. Soheilian, C. Pan, J. R. Barber, Actuating soft matter with magnetic torque. *Adv. Funct. Mater.* **26**, 3859–3880 (2016).
32. A. F. Demirörs, P. P. Pillai, B. Kowalczyk, B. A. Grzybowski, Colloidal assembly directed by virtual magnetic moulds. *Nature* **503**, 99–103 (2013).

33. C. M. Andres, J. Zhu, T. Shyu, C. Flynn, N. A. Kotov, Shape-morphing nanocomposite origami. *Langmuir* **30**, 5378–5385 (2014).
34. E. Z. Meilikhov, R. M. Farzetdinova, Magnetic properties of a random system of rodlike Ising dipoles. *J. Exp. Theor. Phys.* **97**, 593–600 (2003).
35. A. W. Mahoney, J. J. Abbott, Managing magnetic force applied to a magnetic device by a rotating dipole field. *Appl. Phys. Lett.* **99**, 134103 (2011).

Acknowledgments: We acknowledge S. Roh, J. C. Ledford, and L. Reynolds for useful discussions and experimental assistance. **Funding:** This work was supported by the NSF Research Triangle MRSEC (DMR-1121107), NSF grant CBET-1604116, and an NSF graduate research fellowship to C.W.S (GRF-1106401). **Author contributions:** K.H., N.M.D., and C.W.S. performed the assembly experiments directed by O.D.V. C.W.S. fabricated the patchy microcubes under the direction of G.P.L. K.H. analyzed the data following discussion and conceptual guidance by B.B. and O.D.V. B.B. performed the COMSOL simulations. K.H., C.W.S., B.B., G.P.L., and O.D.V contributed to writing of the paper. **Competing interests:** The authors declare that they have no competing interests. **Data and materials availability:** All data needed to evaluate the conclusions in the paper are present in the paper and/or the Supplementary Materials. Additional data are available from authors upon request.

Submitted 8 April 2017
Accepted 30 June 2017
Published 4 August 2017
10.1126/sciadv.1701108

Citation: K. Han, C. W. Shields IV, N. M. Diwakar, B. Bharti, G. P. López, O. D. Velev, Sequence-encoded colloidal origami and microbot assemblies from patchy magnetic cubes. *Sci. Adv.* **3**, e1701108 (2017).

Science Advances

Sequence-encoded colloidal origami and microbot assemblies from patchy magnetic cubes

Koohee Han, C. Wyatt Shields IV, Nidhi M. Diwakar, Bhuvnesh Bharti, Gabriel P. López and Orlin D. Velev

Sci Adv **3** (8), e1701108.
DOI: 10.1126/sciadv.1701108